Research Square

Preprints are preliminary reports that have not undergone peer review.
They should not be considered conclusive, used to inform clinical practice,
or referenced by the media as validated information.

Low-Pressure Investment Casting of Ductile Iron: Effect of Controlled Filling on Graphite Morphology and Fracture Mechanisms

Herman Aleš

ales.herman@fs.cvut.cz

Czech Technical University in Prague

Kopanica Zdeněk

Czech Technical University in Prague

Petr Chytka

IEG Ltd. Jihlava

Novák Vít

Czech Technical University in Prague

Research Article

Keywords: low-pressure investment casting, ductile iron, casting integrity, graphite morphology, fracture mechanism

Posted Date: October 30th, 2026

DOI: https://doi.org/10.21203/rs.3.rs-11220820/v1

License: This work is licensed under a Creative Commons Attribution 4.0 International License.
Read Full License

Additional Declarations: No competing interests reported.

Low-Pressure Investment Casting of Ductile Iron: Effect of Controlled Filling on Graphite Morphology and Fracture Mechanisms

Aleš Herman[1*], Zdeněk Kopanica[1], Petr Chytka[2], Vít Novák[1]

[1] Department of Manufacturing Technology, Faculty of Mechanical Engineering, Czech Technical University in Prague, Technická 4, Prague, Czech Republic

[2] IEG s.r.o., Jihlava, Czech Republic

*Corresponding author: Aleš Herman, ales.herman@fs.cvut.cz

E-mail addresses: Petr Chytka, chytka.p@gmail.com

ORCID: Aleš Herman https://orcid.org/0000-0002-5598-4591; Zdeněk Kopanica https://orcid.org/0009-0001-1199-2354; Petr Chytka https://orcid.org/0009-0009-3350-2916; Vít Novák https://orcid.org/0000-0002-0867-5964

Abstract

This study investigates the effect of low-pressure investment casting (LPIC), a novel process, on the integrity and mechanical properties of ductile iron castings in comparison with conventional gravity investment casting (GIC). Although investment casting is widely used for high-precision components, its application to ductile iron remains limited by turbulence-induced defects and insufficient control of solidification conditions. To eliminate compositional variability, EN-GJS-500 ductile iron castings were produced by both processes from a single melt and evaluated by tensile, Charpy impact and hardness testing, light microscopy and scanning electron microscopy (SEM) of the fracture surfaces. Compared with GIC, LPIC increased the ultimate tensile strength by approximately 22% (from 564 to 687 MPa) and the elongation by approximately 52%, whereas the yield strength and hardness remained comparable. The impact strength decreased by approximately 29%, although with considerably lower scatter. The LPIC castings exhibited a higher nodule count, a smaller mean nodule diameter (28 μm vs. 51 μm) and a more homogeneous graphite distribution. Fractography revealed a transition in the dominant fracture mechanism from graphite nodule fracture in GIC to matrix-controlled failure in LPIC. These findings suggest that the benefits of LPIC extend beyond a reduced defect population and include a modification of the graphite–matrix interaction and load transfer. The combination of laminar filling and pressure-assisted solidification is considered to reduce bifilm formation and enhance feeding. LPIC therefore represents a promising route for improving the performance of ductile iron investment castings in demanding engineering applications.

Keywords low-pressure investment casting; ductile iron; casting integrity; graphite morphology; fracture mechanism

1 Introduction

The demand for high-integrity cast components has increased significantly in recent years owing to stringent requirements on reliability, safety and service life in advanced engineering applications. In this context, casting integrity is understood as the absence of internal defects such as oxide films, inclusions and shrinkage porosity, which are known to critically affect mechanical performance and failure behavior. For ductile iron, whose mechanical properties are strongly governed by graphite morphology and matrix continuity, achieving defect-free microstructures is particularly important [1–5].

Ductile iron is widely used as an engineering material because of its favorable combination of strength, ductility and cost efficiency. These properties result from the formation of spheroidal graphite embedded in a metallic matrix. However, the final performance is highly sensitive to both the metallurgical treatment and the casting conditions, especially melt cleanliness, solidification dynamics and feeding efficiency. Numerous studies have shown that defects such as bifilms and oxide inclusions act as crack initiation sites and significantly reduce tensile properties and ductility. Controlling the melt flow and minimizing turbulence during mold filling are therefore critical factors in improving casting integrity [2–12].

Compared with flake graphite cast iron, the spheroidal graphite in ductile iron provides higher strength, ductility and fracture toughness. The formation and quality of graphite nodules depend strongly on the melt chemistry, magnesium treatment, nucleation conditions and solidification rate. Microstructural parameters, including nodule count, size distribution and matrix constitution, directly influence the resulting mechanical properties. At the same time, defects such as oxide films, inclusions, bifilms and shrinkage porosity act as stress concentrators and markedly deteriorate tensile and impact performance. Consequently, high melt cleanliness and controlled mold filling are essential for producing ductile iron castings with high structural integrity and reliability [1, 3, 4, 7–9, 11–13].

The metallurgical treatment of the melt further contributes to the final casting quality. Conventional MgFeSi nodularizing alloys often produce highly exothermic reactions, generating slag, oxide inclusions and turbulent melt motion that may compromise melt cleanliness. In contrast, FeNiMg nodularizing alloys provide more stable magnesium dissolution, lower reaction intensity, reduced slag formation and improved resistance to magnesium fading. To moderate the reactivity of conventional treatments, MgFeSi alloys containing calcium and rare earth elements have been developed, and the selection of the treatment alloy, together with the inoculant, has been shown to influence graphite morphology and mechanical properties, particularly in castings of varying section size. The combination of a cleaner melt, controlled filling dynamics and pressure-assisted solidification creates favorable conditions for uniform graphite nucleation and growth, resulting in a more homogeneous graphite distribution and fewer casting defects. These improvements are generally expected to increase tensile strength and ductility, because they reduce the occurrence of bifilms, porosity and oxide-related defects, which are widely recognized as major fracture initiation sites in cast alloys [2, 4, 7–9, 11, 14–17].

Investment casting offers significant advantages in terms of dimensional accuracy, surface quality and the ability to produce complex geometries. For ferrous alloys, however, the process is predominantly based on gravity filling (gravity investment casting, GIC), which inherently involves free-fall, turbulent metal flow, air entrainment and oxide formation. These effects are particularly critical for ductile iron, in which even small amounts of entrained oxides may disrupt graphite nucleation and growth and increase the risk of microshrinkage, leading to heterogeneous microstructures, reduced nodularity and an increased defect population. As a result, despite its technological advantages, investment casting of ductile iron remains limited in applications requiring the highest structural integrity [2, 4–6, 10, 18, 19].

In contrast, low-pressure die casting (LPDC), which is widely used for aluminum alloys, enables controlled bottom-up mold filling with a laminar flow regime, significantly reducing oxide entrainment and bifilm formation. Furthermore, the application of pressure during solidification improves feeding efficiency and suppresses shrinkage-related defects. While these principles have been extensively validated for low-melting-point alloys,

their application to high-temperature ferrous systems remains largely unexplored because of the technological challenges associated with melt handling and refractory materials [20–25].

Low-pressure casting is well established in the production of aluminum alloy castings, a typical example being cast aluminum wheels, and is used for casting into both metal molds and molds made of self-hardening molding mixtures. Another technology used mainly for aluminum alloys is counter-pressure casting, in which the metal is drawn into a shell placed in a vacuum chamber. However, low-pressure casting of alloys with higher melting points (e.g., Ni alloys, Co alloys and Fe alloys) is not commercially available [18, 22–25].

To address this limitation, a novel hybrid process, low-pressure investment casting (LPIC), has been developed, combining the ceramic shell molds typical of investment casting with the controlled melt delivery characteristic of LPDC. By filling the mold from the bottom under controlled pressure, LPIC promotes a smooth laminar flow, minimizes oxide entrainment and improves feeding during solidification. The applied pressure enhances liquid metal transport within interdendritic regions, reducing shrinkage-related defects and improving the homogeneity of the final microstructure. In addition, controlled filling conditions may help stabilize graphite crystallization, support higher nodule counts, improve nodularity and reduce the undercooling sensitivity commonly observed in thin-walled ductile iron castings. The key assumption is that controlled metal flow and solidification under slight overpressure fundamentally alter the mechanisms of defect formation and graphite crystallization [2–4, 6, 8–10, 12, 20–23, 25].

Despite the potential of this concept, systematic experimental studies evaluating the effect of low-pressure filling on ductile iron cast in ceramic shells are lacking, particularly with respect to the relationship between microstructure, defect population and fracture mechanisms. Existing research on ductile iron investment casting focuses primarily on process optimization through simulation and on alloy composition, whereas the influence of controlled filling dynamics remains insufficiently understood [3, 8, 9, 12, 18, 22–24].

The aim of this study is therefore to investigate the effect of LPIC technology on the integrity and mechanical properties of ductile iron castings in comparison with conventional GIC. The study is based on a controlled experimental design using a single melt of identical chemical composition, allowing a direct comparison of the two technologies. Particular attention is given to the relationship between graphite morphology, defect population and fracture behavior.

The central hypothesis of this work is that LPIC technology, through controlled laminar filling and pressure-assisted solidification, suppresses bifilm formation and modifies the graphite–matrix interaction, resulting in a shift in the dominant fracture mechanism from graphite-controlled to matrix-controlled failure. This change is expected to lead to a significant improvement in tensile strength and ductility, while potentially influencing impact toughness.

The main contributions of this paper are as follows:

- demonstration of the applicability of low-pressure casting principles to high-temperature ductile iron investment casting;
- experimental quantification of the improvements in mechanical properties and casting integrity;
- identification of a change in the fracture mechanism associated with modified graphite behavior;
- establishment of a process–structure–property relationship for LPIC technology.

2 Materials and Methods

2.1 LPIC Equipment

A complete low-pressure machine for casting into ceramic shell molds produced by investment casting technology was developed. The main technical challenges were a special connection between the shell and the riser tube, a riser tube material resistant to temperatures of up to 1800 °C, and a special shut-off valve enabling rapid shell handling. After the machine had been built, suitable process parameters for the low-pressure casting of various alloys were established. A filled shell on the LPIC machine is shown in Fig. 1.



Fig. 1 Filled ceramic shell on the LPIC machine

2.2 Material and Test Specimens

Test castings of EN-GJS-500 ductile iron produced by LPIC were compared with castings produced by conventional GIC. To eliminate compositional variability, both variants were cast from a single melt; its chemical composition is given in Table 1.

Table 1 Chemical composition of the EN-GJS-500 melt (wt.%)

Element	C	Si	Mn	P	S	Ni	Mg	CE
Content (wt.%)	3.55	2.42	0.146	0.0278	0.0110	0.10	0.0463	4.36

CE, carbon equivalent

Specimens for Charpy impact testing and tensile testing were cast, and the ultimate tensile strength R_m, the 0.2% proof stress $R_{p0.2}$, the uniform elongation A_g and the elongation after fracture A were determined. The geometries of the Charpy V-notch specimen (10 × 10 × 55 mm, notch depth 2 mm) and of the tensile specimen (gauge diameter 10 mm, parallel length 56 mm) are shown in Fig. 2; the drawings give nominal dimensions, and a casting shrinkage

of 3% was taken into account in the pattern design. The specimens were attached to the casting tree as shown in Fig. 3. At the technology validation stage, each casting tree carried 18 tensile and 18 impact test specimens.

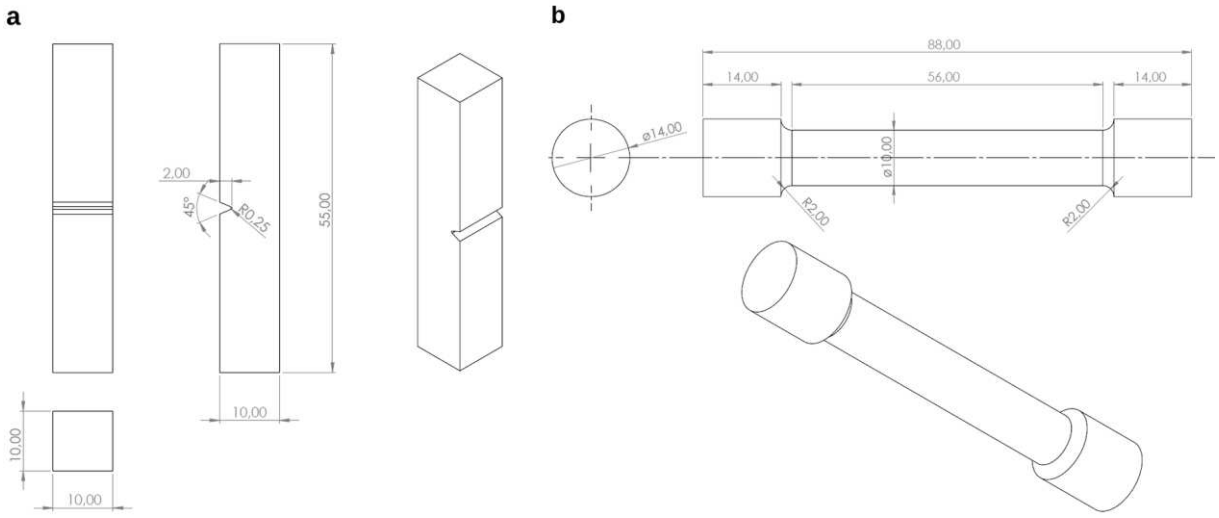


Fig. 2 Test specimens (nominal dimensions in mm): (**a**) Charpy V-notch impact test specimen; (**b**) tensile test specimen

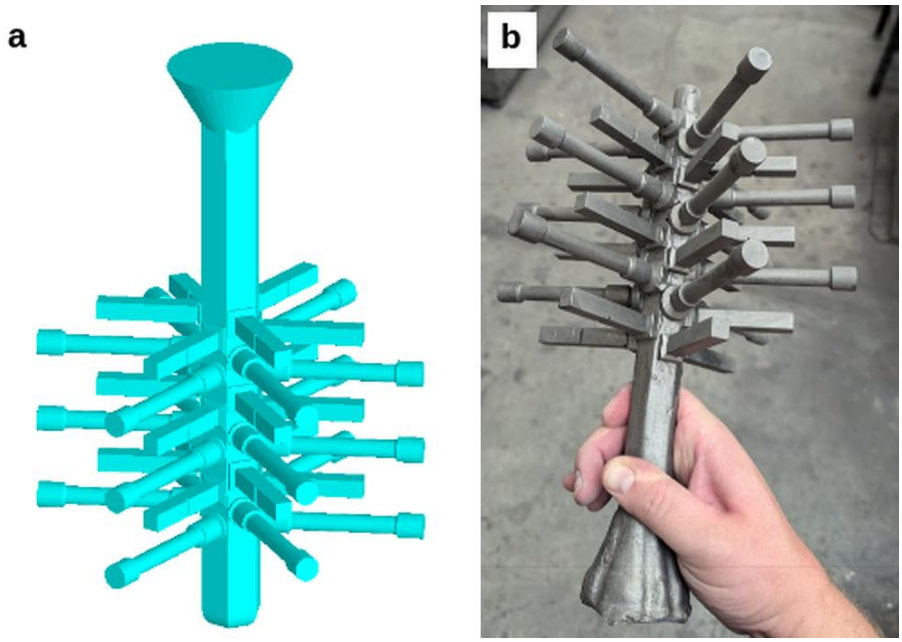


Fig. 3 Casting tree with test specimens: (**a**) 3D model (overall dimensions: diameter 222 mm, total height including the pouring cup 310 mm); (**b**) cast tree

Specimens with a crack in the neck or with markedly outlying results (minimum and maximum values) were excluded from the evaluation; consequently, the mean values were calculated from seven or eight valid specimens per condition (Sect. 3.3). In addition to the elongation after fracture A, the uniform elongation A_g (plastic elongation at maximum force) was evaluated, because the difference between these two values reflects the internal homogeneity of the material. The $R_{p0.2}/R_m$ ratio, which in a certain sense represents the plasticity reserve of the material, was also considered. Brinell hardness (HB) was determined for both variants. The influence of the specimen position on the individual tiers of the casting tree on the mechanical properties was also examined.

For comparison with conventional castings, i.e., castings produced not in a ceramic shell but in a sand mold with substantially greater wall thicknesses, a standard Y-block test casting according to EN 1563 [26] was cast by gravity into a cold-box sand mold.

2.3 Ceramic Shell Molds

The ceramic shell molds for both GIC and LPIC were produced by the same investment casting procedure. The two face coats consisted of an ethanol-based sol–gel binder with silica (SiO_2) flour and were stuccoed with silica (SiO_2); the backup coats were produced from the same slurry and stucco materials. In total, seven layers were applied, giving a shell thickness of approximately 9 mm. Before casting, the shells were dewaxed, fired and preheated to the mold temperature defined in the design of experiments (DoE; 850–950 °C); the GIC and LPIC shells compared in this study were preheated to the same temperature of 900 °C.

2.4 Metallographic and Fractographic Evaluation

Metallographic sections were prepared from the Charpy impact test specimens using standard metallographic procedures. Graphite morphology (nodule count, nodularity, mean nodule diameter and shape factor) was evaluated by automated image analysis on unetched sections according to ISO 945-4 [27] and ISO 945-1 [28]; graphite particles smaller than 5 µm were excluded from the evaluation. The matrix was subsequently revealed by etching with 2% nital. The fracture surfaces of the Charpy impact test specimens were examined by scanning electron microscopy (SEM).

2.5 Process Optimization and Statistical Analysis

To optimize the process parameters, a DoE was created with the following basic variables: pouring temperature, mold filling time, filling pressure and mold temperature. The optimal parameters were determined by the following procedure:

(1) numerical simulation was used to determine the range of initial process conditions;
(2) based on the simulation results, extreme and intermediate conditions were selected for experimental verification;
(3) a DoE was designed for these conditions;
(4) eight casting trees were cast by LPIC according to the DoE parameters, and a mathematical model was derived from the results to determine the optimal parameters.

Mean values are reported together with their standard deviations (SD). The statistical significance of the differences between GIC and LPIC was assessed using a two-tailed Welch's *t*-test at a significance level of 0.05.

3 Results

3.1 Nodularizing Treatment and Microstructure

Fine-tuning of the metallurgical process involved adapting the nodularizing treatment, refining and inoculation of the melt so that the reaction would not be too violent, even for the small volume of molten metal and under the confined conditions of a low-pressure casting machine. The main challenge was the implementation of the nodularizing treatment, because treatments using current MgFeSi nodularizing alloys are highly reactive, which is dangerous in the confined space of the LPIC machine. Based on operational tests, a historical FeNiMg treatment

alloy (first used in the production of ductile iron castings in 1947 [14]) was selected, as it produced the least violent reaction (Fig. 4). The treatment alloys, housed in a 0.1 mm thick steel sheet casing attached to a steel wire, were introduced into the melt by immersion (Fig. 5). Lower-reactivity MgFeSi treatment alloys containing Ca and rare earth elements [15–17] were considered but deliberately not used. Calcium-bearing treatment alloys increase the amount of slag and non-metallic inclusions in the melt and may therefore become a source of casting defects, which would contradict the primary aim of the LPIC process, i.e., maximum melt cleanliness. In addition, the nickel introduced with the FeNiMg alloy was beneficial for the target microstructure: as a graphitizing element that strengthens ferrite in solid solution, nickel supports the formation of a ferritic–pearlitic matrix while still providing the strength level required for EN-GJS-500.

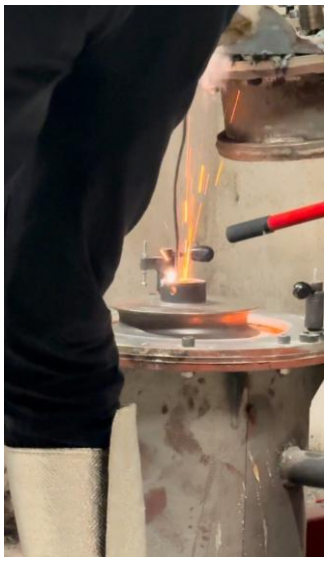


Fig. 4 Nodularizing treatment in the melting crucible under the lid



Fig. 5 Steel sheet casing containing the treatment alloy and inoculant

The refined treatment procedure for a 16 kg furnace charge was as follows: nodularizing treatment with an FeNiMg alloy (35% Ni, 5–6% Mg, balance Fe) in an amount of 1.25% (200 g); inoculation with a Ba-bearing FeSi75 inoculant in an amount of 0.6% (60 g); and addition of DESULCO carbon raiser with an inoculating effect in an amount of 0.2% (20 g). All additions were placed in a 0.1 mm thick steel container fitted with a secured immersion wire. This procedure resulted in a nodularity of 87–88% across the cross-section in all cases (Table 2) and was therefore used for all experiments within the DoE.

The microstructures of the GIC and LPIC castings are compared in Fig. 6, and the graphite morphology parameters are summarized in Table 2. In the unetched state, the GIC castings show a relatively large variation in graphite nodule size, whereas the LPIC castings exhibit a finer and more uniform graphite distribution. The mean nodule diameter decreased from 51 µm (GIC) to 28 µm (LPIC), the nodule count increased from 120 to 140 nodules/mm^2, and the shape factor increased from 0.86 to 0.90, while the nodularity remained practically unchanged (87% and 88%).

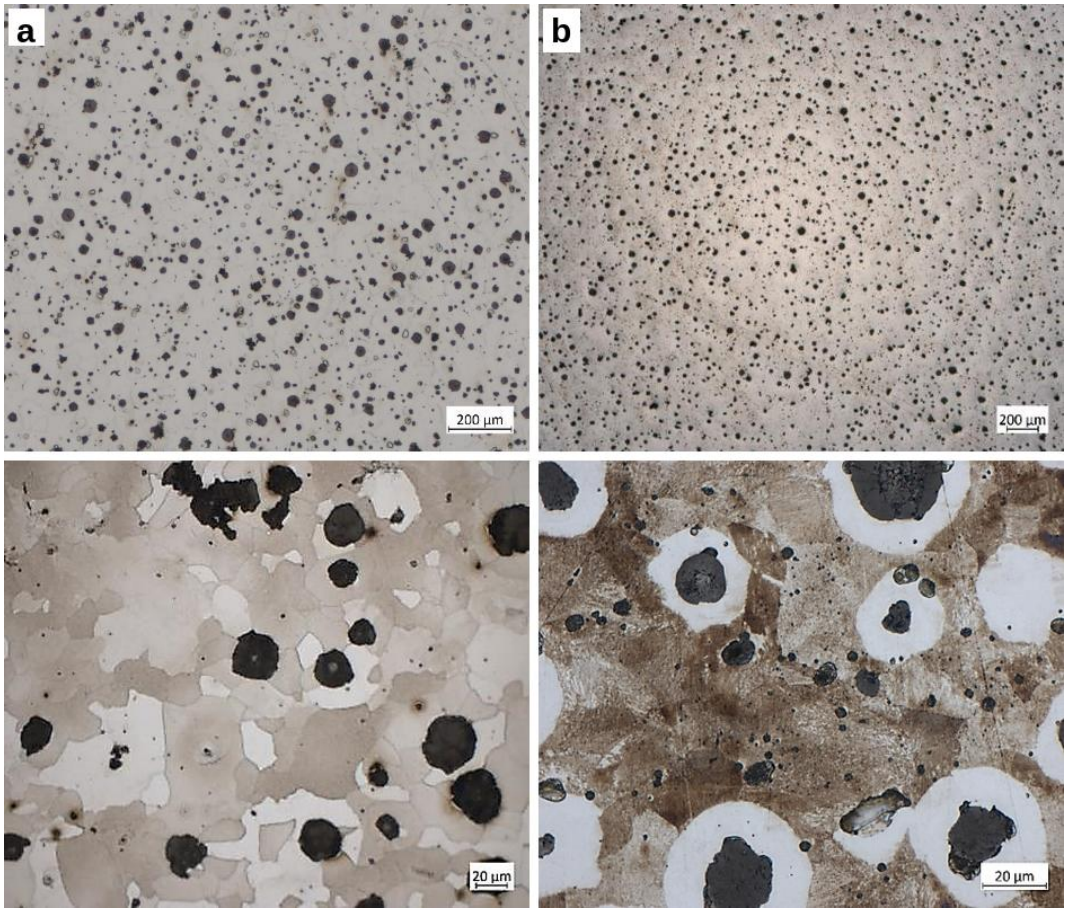


Fig. 6 Microstructure of EN-GJS-500 castings: (**a**) GIC; (**b**) LPIC. Light microscopy; top row unetched (original magnification 50×, scale bar 200 µm), bottom row etched with 2% nital (original magnification 500×, scale bar 20 µm)

Table 2 Graphite morphology parameters of the GIC and LPIC castings evaluated according to ISO 945-1 and ISO 945-4 [27, 28]

Parameter	GIC	LPIC
Nodule count (nodules/mm^2)	120	140
Nodularity (%)	87	88
Mean nodule diameter (µm)	51	28
Shape factor (–)	0.86	0.90

3.2 Process Optimization

Numerical simulations (Fig. 7) were used to determine the process boundary parameters, which were then used as baseline values for the DoE. The DoE covered the following process window: pouring temperature 1260–1340 °C, mold temperature 850–950 °C, filling time 1.5–3 s and filling pressure 0.13–0.15 MPa. The parameters that

yielded the best mechanical properties were a pouring temperature of 1280 °C, a mold temperature of 900 °C, a filling time of 3 s and a filling pressure of 0.144 MPa. Given the broad scope of the experimental program, only the results obtained with these optimal parameters are presented below.

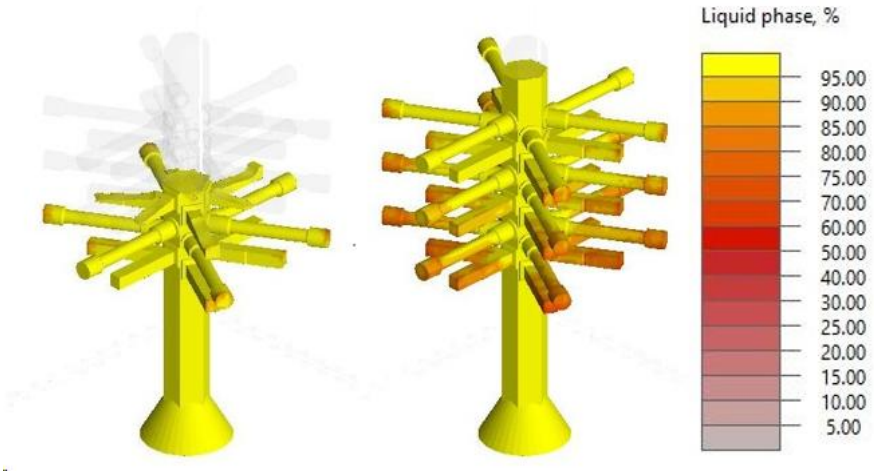


Fig. 7 Numerical simulation of the solidification of the EN-GJS-500 casting tree (liquid phase fraction, %)

3.3 Mechanical Properties

The individual tensile test results for the GIC and LPIC castings are listed in Tables 3 and 4, the Charpy impact test results in Table 5, and the mean values of all mechanical properties, including hardness, are compared in Table 6. Overall, the mechanical test results reveal a consistent and statistically significant improvement in the tensile performance of the LPIC castings compared with GIC.

Table 3 Tensile test results of the gravity investment castings (GIC), EN-GJS-500

Specimen	E (GPa)	$R_{p0.2}$ (MPa)	R_m (MPa)	A_g (%)	A (%)
1	199	347	558	1.65	1.77
2	226	327	555	1.45	1.51
3	213.8	373	548	2.83	2.94
4	201	460	572	2.22	2.34
5	192	332	562	7.15	7.40
6	205	298	608	4.74	4.90
7	220	400	565	4.52	4.68
8	215	314	546	6.64	6.89
Mean	209	356	564	3.90	4.05
SD	10.8	49.6	18.4	2.07	2.13

SD, standard deviation

Table 4 Tensile test results of the low-pressure investment castings (LPIC), EN-GJS-500

Specimen	E (GPa)	$R_{p0.2}$ (MPa)	R_m (MPa)	A_g (%)	A (%)
1	228.6	377	666	4.15	4.21
2	227.8	260	690	7.27	7.36
3	210.6	399	680	5.28	5.38
4	181.7	309	692	6.82	6.95
5	223.6	298	693	5.61	5.70
6	209.2	388	697	6.69	6.77
7	226.1	368	693	6.61	6.67
Mean	215	343	687	6.06	6.15
SD	15.6	49.3	10.0	1.01	1.02

SD, standard deviation

Table 5 Charpy V-notch impact test results, EN-GJS-500

Specimen	KCV, GIC (J/cm^2)	KCV, LPIC (J/cm^2)
1	7	5
2	7	6
3	6	6
4	6	5.5
5	8.5	5.5
6	9	5.5
7	11.5	6.5
8	11.5	7.5
Mean	8.3	5.9
SD	2.09	0.73

SD, standard deviation

Table 6 Comparison of the mean mechanical properties and impact strength of the GIC and LPIC castings, EN-GJS-500

	E (GPa)	$R_{p0.2}$ (MPa)	R_m (MPa)	A_g (%)	A (%)	HB	KCV (J/cm^2)
GIC	209 ± 11	356 ± 50	564 ± 18	3.9 ± 2.1	4.1 ± 2.1	218 ± 11	8.3 ± 2.1
LPIC	215 ± 16	343 ± 49	687 ± 10	6.1 ± 1.0	6.1 ± 1.0	220 ± 6	5.9 ± 0.7
LPIC/GIC (%)	103	96	122	155	152	101	71

Values are given as mean ± SD

The mean ultimate tensile strength R_m increased from 564 ± 18 MPa (GIC) to 687 ± 10 MPa (LPIC), corresponding to an improvement of approximately 22% ($p < 0.001$). At the same time, the elongation after fracture A increased from 4.1 ± 2.1% to 6.1 ± 1.0%, representing an increase of approximately 52% ($p < 0.05$). The 0.2% proof stress $R_{p0.2}$ remained statistically comparable for the two technologies (356 ± 50 MPa for GIC vs. 343 ± 49 MPa for LPIC; $p > 0.5$); consequently, the $R_{p0.2}/R_m$ ratio decreased from 0.63 (GIC) to 0.50 (LPIC). This indicates that the improvement occurs primarily in the strain hardening capacity and ductility rather than in the onset of plastic deformation. Importantly, the standard deviations of the key properties, particularly the tensile strength and elongation, are markedly lower for the LPIC castings, suggesting improved process stability and structural homogeneity.

In contrast to the tensile properties, the impact strength KCV decreased from 8.3 ± 2.1 J/cm^2 (GIC) to 5.9 ± 0.7 J/cm^2 (LPIC), corresponding to a statistically significant reduction of approximately 29% ($p < 0.05$). The

hardness remained practically unchanged, at 218 ± 11 HB (GIC) and 220 ± 6 HB (LPIC), indicating that the overall matrix strength is comparable for the two casting technologies.

For comparison, the properties of the standard sand-cast Y-block are given in Table 7. Owing to its substantially larger section thickness, the Y-block exhibited a lower tensile strength but considerably higher elongation and impact strength than both investment-cast variants. The improvements in the tensile properties of the LPIC castings correlate with the refined graphite morphology and with the reduced defect population identified by the metallographic and fractographic analyses.

Table 7 Mechanical properties of the sand-cast Y-block test casting according to EN 1563 [26]

	E (GPa)	$R_{p0.2}$ (MPa)	R_m (MPa)	A_g (%)	A (%)	HB	KCV (J/cm^2)
Y-block	212 ± 14	303 ± 12	458 ± 15	26 ± 3	27 ± 4	178 ± 14	16 ± 2

Values are given as mean ± SD

3.4 Fractography

SEM overviews of the fracture surfaces of the Charpy impact test specimens are shown in Fig. 8. The aim of the fracture surface analysis was to determine whether the higher strength of the LPIC castings can be attributed solely to the finer graphite structure and its more uniform distribution, i.e., to the higher number of nucleation sites per unit area.

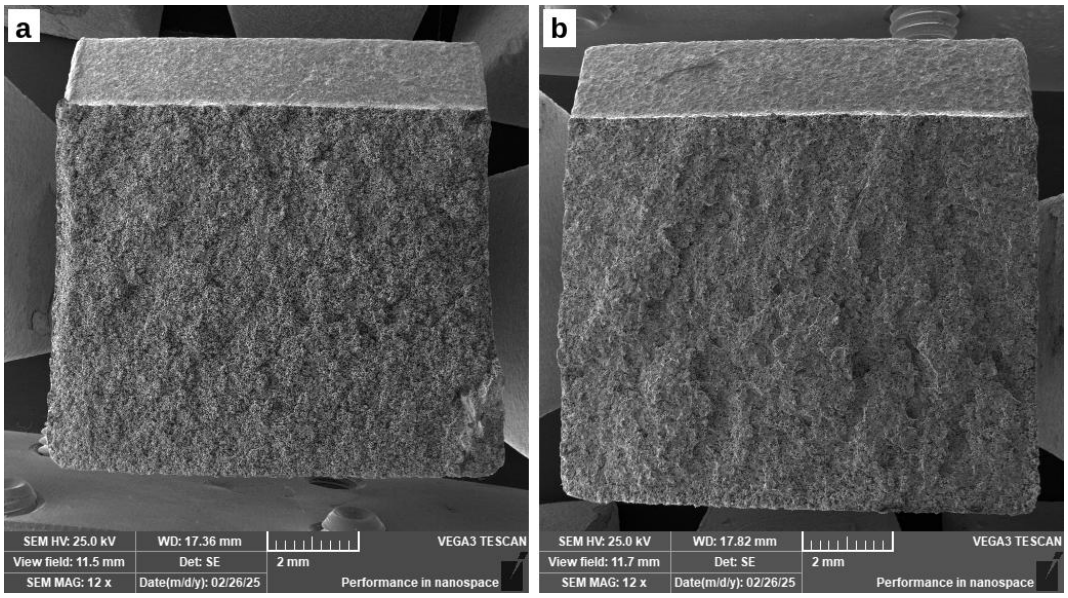


Fig. 8 SEM overview of the fracture surfaces of the Charpy impact test specimens: (**a**) GIC; (**b**) LPIC

A detailed analysis revealed a higher proportion of ductile fracture and a lower proportion of brittle fracture on the GIC fracture surfaces, whereas the proportion of brittle fracture on the LPIC fracture surfaces was approximately 10–15% higher (Fig. 9). Specimens corresponding to the minimum, maximum and mean values of the impact test results were examined; the figures show the specimens corresponding to the mean values. While this finding is consistent with the results of the impact tests, it does not explain the increase in strength.

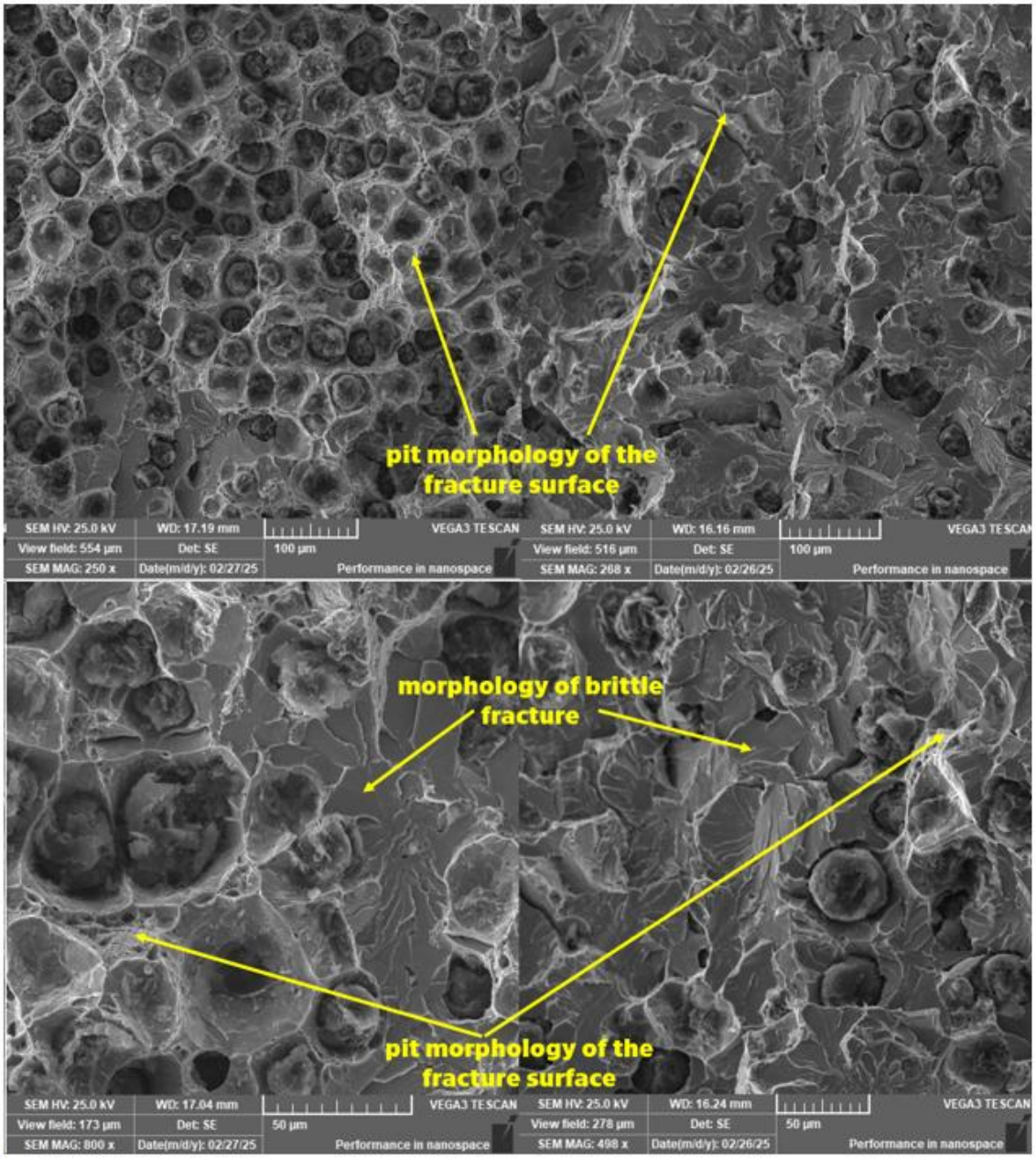


Fig. 9 Brittle and ductile fracture regions on the fracture surfaces at different magnifications; left column GIC, right column LPIC

The analysis therefore focused on the regions surrounding the graphite nodules. A pronounced difference between GIC and LPIC was found in the damage of the graphite nodules (Fig. 10). In the GIC specimens, most graphite nodules appear to be fractured, and occasional slight indentations along the nodule edges indicate that the surrounding matrix was torn away (Fig. 10, left). In contrast, the LPIC specimens exhibit a different damage mechanism: the vast majority of graphite nodules remain intact, while the surrounding matrix is torn away to a relatively large depth (Fig. 10, right; detail in Fig. 11). This suggests that solidification under slight overpressure alters the strength of the graphite nodules, so that the matrix surrounding them fails before the nodules themselves are damaged. This change in the damage mechanism is considered the main reason for the superior tensile strength and ductility of the LPIC castings.

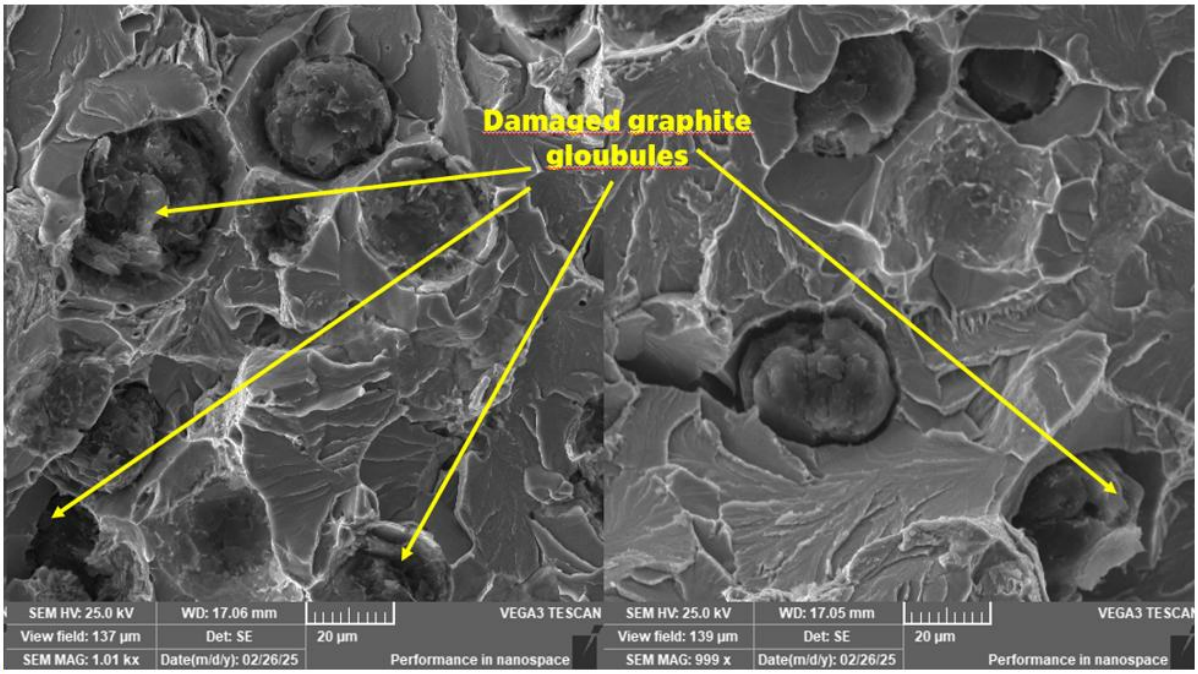


Fig. 10 Damage to the graphite nodules on the fracture surfaces (SEM); left GIC, right LPIC

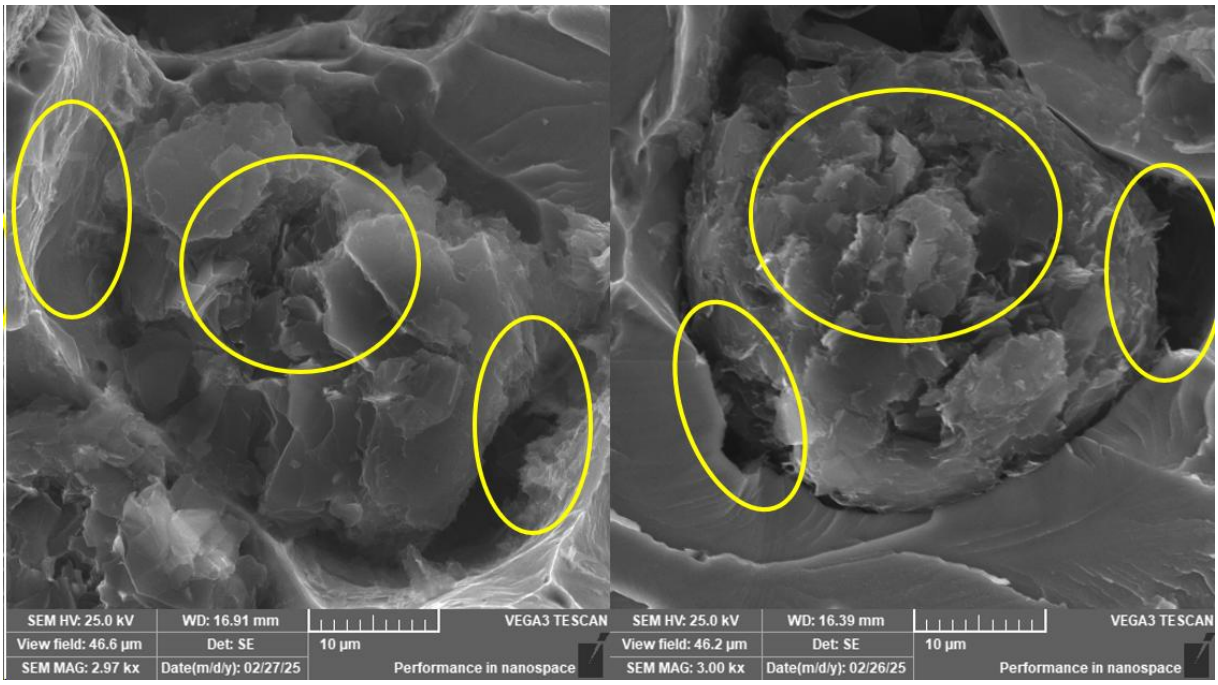


Fig. 11 Detail of the damage to the graphite nodules (SEM); left GIC, right LPIC

4 Discussion

The results of this study demonstrate that the LPIC process leads to a significant improvement in tensile strength and ductility compared with conventional GIC while maintaining comparable hardness, at the cost of a significant reduction in impact strength (approximately 29%). These findings indicate that the effect of LPIC is not limited to microstructural refinement but involves a more fundamental modification of the defect formation mechanisms and load transfer behavior within the material.

4.1 Influence of Filling Dynamics and Melt Cleanliness

One of the key differences between LPIC and GIC lies in the mold filling mode. In GIC, the free-fall filling mechanism inherently introduces turbulence, resulting in air entrainment and the formation of oxide bifilms. These defects are well established as critical crack initiation sites that significantly reduce mechanical performance [2, 4–6, 10, 19].

In contrast, LPIC employs controlled bottom-up filling under low and stable pressure, promoting a near-laminar flow regime and minimizing melt–air interaction. The observed increases in ultimate tensile strength (approximately 22%) and elongation (approximately 52%) of the LPIC castings are consistent with a reduced population of such defects. Furthermore, the reduced scatter (lower standard deviation) of the mechanical properties indicates improved structural homogeneity and melt cleanliness [2, 4, 22, 23, 25].

These observations agree with bifilm theory, which identifies oxide films as one of the most detrimental defect types governing the tensile behavior of cast alloys. However, the magnitude of the observed improvement suggests that the influence of LPIC extends beyond defect suppression alone [2, 4–6, 10, 19].

4.2 Microstructure: Graphite Morphology and Distribution

Metallographic analysis revealed a significant refinement of the graphite morphology in the LPIC castings. The reduction in mean nodule diameter (from 51 μm to 28 μm), together with the increase in nodule count (from 120 to 140 nodules/mm^2), suggests a higher nucleation density and a more uniform graphite distribution. This effect can be attributed to improved melt cleanliness, reduced turbulence during filling and modified solidification conditions under the applied pressure [3, 8, 9, 11, 12].

A higher density of smaller graphite nodules reduces local stress concentration and promotes a more uniform stress distribution within the matrix, which directly contributes to the observed increase in tensile strength and ductility. Additionally, the more homogeneous microstructure reduces the spatial variability of solidification conditions, further improving the reproducibility of the mechanical properties [1, 3, 8, 9, 11–13].

4.3 Fracture Mechanism: Transition from Graphite-Controlled to Matrix-Controlled Failure

A key finding of this study, supported by SEM fracture analysis, is the change in the dominant fracture mechanism between the GIC and LPIC castings. In the GIC castings, the fracture surfaces exhibit a high proportion of fractured graphite nodules, indicating that failure is strongly influenced by stress localization at the graphite–matrix interfaces and by internal defects. The premature fracture of graphite nodules suggests a limited load transfer capability and defect-driven crack initiation [29–32].

In contrast, the LPIC castings show markedly different behavior: the majority of graphite nodules remain intact, while failure occurs predominantly in the surrounding matrix. This observation indicates a shift in the load transfer mechanism, in which the graphite nodules no longer represent the primary weak points of the structure [30–32].

This transition from graphite-controlled to matrix-controlled fracture represents a fundamental change in material behavior. It provides a mechanistic explanation for the observed improvement in tensile properties and suggests that LPIC modifies the graphite–matrix interaction, enabling more effective stress redistribution and delaying crack initiation [1, 13, 29–32].

4.4 Effect of Pressure on Solidification and Feeding

An additional factor associated with LPIC is the application of pressure during solidification. Even a relatively low overpressure can enhance feeding in the mushy zone, thereby reducing the formation of microshrinkage and improving the continuity of the metallic matrix [3, 20–23, 25].

In ductile iron, where the eutectic graphite expansion partially compensates for shrinkage, the feeding conditions remain complex and highly sensitive to local solidification dynamics. Insufficient feeding can result in microvoids and porosity, which negatively affect ductility and fatigue resistance [3, 8, 9, 12].

The pressure applied in LPIC is likely to stabilize the solidification front and enhance liquid metal transport within interdendritic regions, resulting in a more coherent microstructure. This mechanism complements the improvement in melt cleanliness and contributes to the overall increase in mechanical performance [3, 20–23, 25].

4.5 Trade-off Between Strength and Impact Toughness

Despite the significant improvement in tensile properties, a statistically significant reduction in impact strength (KCV) of approximately 29% was observed for the LPIC castings. This behavior is consistent with the fractographic observations, which indicate an increased proportion of brittle fracture features. Several factors may contribute to this trend:

- microstructural refinement associated with higher strength;
- increased matrix constraint due to the reduced defect population;
- the transition to matrix-controlled fracture, which may limit plastic deformation ahead of the crack tip.

This behavior partly reflects the strength–toughness trade-off commonly observed in metallic materials. Notably, however, the reduction in KCV occurred despite the increase in tensile elongation, which suggests that notched dynamic loading is more sensitive than quasi-static tension to the matrix-controlled fracture mode observed in the LPIC castings. In relative terms, the loss of impact strength is comparable to the gain in ultimate tensile strength and cannot be regarded as negligible. LPIC therefore appears most suitable for components loaded predominantly under quasi-static conditions, where strength and reproducibility of properties are prioritized, whereas its application to impact-loaded components requires further evaluation. At the same time, the markedly lower scatter of the KCV values for LPIC (±0.7 vs. ±2.1 J/cm^2) indicates more reproducible impact behavior [1, 3, 13, 29].

4.6 Comparison with Existing Approaches

Most existing studies on ductile iron investment casting focus on incremental improvements through process simulation, alloy design and inoculation strategies. While these approaches can enhance the microstructure and reduce defect formation, they do not fundamentally modify the mold filling dynamics [3, 7–9, 11, 12].

In contrast, LPIC introduces a process-level innovation that directly addresses one of the primary sources of defects, i.e., turbulent melt flow during mold filling. Analogous approaches, such as low-pressure die casting and counter-pressure casting, have been successfully implemented for aluminum alloys, where improved filling control leads to enhanced casting integrity [22, 23, 25].

The present results demonstrate that these principles can be successfully transferred to high-temperature ferrous systems, specifically to ductile iron cast in ceramic shell molds. This represents a shift from incremental optimization toward a more fundamental redesign of the casting process, in which melt flow, solidification behavior and defect formation are controlled simultaneously [18, 24].

4.7 Limitations and Future Work

Although the results are promising, several limitations should be acknowledged:

- the study is limited to a single alloy (EN-GJS-500);
- the matrix constitution (ferrite/pearlite fraction) and the nodule size distribution were not quantified;
- further statistical validation on a larger number of specimens and casting trees could strengthen the robustness of the conclusions;
- the reduction in impact strength is not yet fully explained; instrumented impact testing and quantification of the ferrite/pearlite fraction are needed to clarify its origin.

Initial trials with EN-GJS-400, EN-GJS-500, EN-GJS-600 and EN-GJS-700 castings, which are not reported here, indicated that LPIC achieves tensile strengths at least 20% higher than those obtained by gravity casting. Future research should therefore focus on:

- extending the LPIC process to higher-strength ductile iron grades;
- quantitative characterization of the matrix phase fractions and nodule size distributions;
- advanced defect analysis (e.g., X-ray computed tomography);
- modeling of pressure-assisted solidification and graphite nucleation;
- evaluation of lower-reactivity Ca- and RE-bearing MgFeSi treatment alloys under LPIC conditions [15–17].

5 Conclusions

This study demonstrates that the low-pressure investment casting (LPIC) process can be successfully applied to ductile iron castings produced in ceramic shell molds and offers significant advantages over conventional gravity investment casting (GIC). By combining controlled bottom-up filling with pressure-assisted solidification, LPIC fundamentally modifies the casting conditions responsible for defect formation, graphite development and fracture behavior. The main conclusions are as follows:

(1) Compared with GIC, LPIC increased the ultimate tensile strength from 564 ± 18 MPa to 687 ± 10 MPa (approximately 22%) and the elongation from 4.1 ± 2.1% to 6.1 ± 1.0% (approximately 52%). The yield strength and hardness remained essentially unchanged, whereas the impact strength decreased by approximately 29%, from 8.3 ± 2.1 to 5.9 ± 0.7 J/cm^2, albeit with markedly lower scatter. The lower scatter of the tensile properties of the LPIC castings indicates improved process stability and greater structural homogeneity.

(2) Metallographic examination revealed a substantial refinement of the graphite morphology, with the mean nodule diameter decreasing from 51 µm (GIC) to 28 µm (LPIC) and the nodule count increasing from 120 to 140 nodules/mm^2. The more uniform distribution of graphite nodules is attributed to improved melt cleanliness, reduced turbulence and enhanced solidification conditions under pressure, which contribute to a reduced defect population and a more efficient stress distribution within the metallic matrix.

(3) The most significant finding of this work is the change in the dominant fracture mechanism. SEM fractography showed that failure of the GIC castings is largely associated with fractured graphite nodules, whereas the LPIC castings exhibit predominantly intact nodules surrounded by fractured matrix. This transition from graphite-controlled to matrix-controlled fracture indicates an improved graphite–matrix interaction and more effective load transfer. The enhanced tensile performance of the LPIC castings

therefore cannot be explained solely by defect reduction or graphite refinement but must also be attributed to a fundamental change in the failure mechanism.

(4) The results confirm the central hypothesis that controlled laminar filling and pressure-assisted solidification suppress defect formation and modify the mechanical response of ductile iron castings. LPIC thus represents a promising process innovation capable of extending the application of investment-cast ductile iron components in demanding engineering sectors where high strength, reliability and structural integrity are required.

Future work should focus on the quantitative characterization of defect populations and matrix constitution, validation on higher-strength ductile iron grades, and detailed modeling of pressure-assisted graphite nucleation and solidification.

Declarations

Funding

The experimental work was carried out within project No. FW06010093, supported by the Technology Agency of the Czech Republic under the TREND programme. Data evaluation and preparation of the manuscript were supported by the Student Grant Competition of the Czech Technical University in Prague, project No. SGS25/133/OHK2/3T/12 “Technologies and materials for energetics produced by additive and foundry processes”.

Competing Interests

Petr Chytka is an employee of IEG s.r.o., Jihlava, Czech Republic, which developed the LPIC casting equipment used in this study and commercially offers the equipment and licences for the LPIC technology. The other authors declare no competing interests.

Author Contributions

All authors contributed to the study conception and design, the experimental work, data analysis and interpretation, and the preparation of the manuscript. All authors read and approved the final manuscript.

Data Availability

The datasets generated and analyzed during the current study are available from the corresponding author on reasonable request.

Ethics Approval

Not applicable.

References

1. Z.-H. Wang, X. Zhang, F.-L. Xu, K.-C. Qian, K.-M. Chen, Effect of nodularity on mechanical properties and fracture of ferritic spheroidal graphite iron. China Foundry **16**, 386–392 (2019). https://doi.org/10.1007/s41230-019-9080-z
2. J. Campbell, An overview of the effects of bifilms on the structure and properties of cast alloys. Metall. Mater. Trans. B **37**, 857–863 (2006). https://doi.org/10.1007/BF02735006
3. D.M. Stefanescu, *Science and Engineering of Casting Solidification*, 3rd edn. (Springer, Cham, 2015). https://doi.org/10.1007/978-3-319-15693-4
4. J. Campbell, *Complete Casting Handbook: Metal Casting Processes, Metallurgy, Techniques and Design*, 2nd edn. (Butterworth-Heinemann, Amsterdam, 2015)

5. J. Campbell, *Castings: The New Metallurgy of Cast Metals*, 2nd edn. (Butterworth-Heinemann, Burlington, MA, 2003)
6. M.A. El-Sayed, The behaviour of bifilm defects in cast Al-7Si-Mg alloy. PLoS ONE **11**, e0160633 (2016). https://doi.org/10.1371/journal.pone.0160633
7. I. Kiss, Comparative study on the in-ladle treatment techniques for nodulizing the iron's graphite. Teh. Glas. **15**, 504–509 (2021). https://doi.org/10.31803/tg-20210209111953
8. I. Riposan, E. Stefan, S. Stan, N.R. Pana, M. Chisamera, Effects of inoculation on structure characteristics of high silicon ductile cast irons in thin wall castings. Metals **10**, 1091 (2020). https://doi.org/10.3390/met10081091
9. K.M. Pedersen, N.S. Tiedje, Undercooling and nodule count in thin walled ductile iron castings. Int. J. Cast Met. Res. **20**, 145–150 (2007). https://doi.org/10.1179/136404607X239816
10. M.A. El-Sayed, K. Essa, H. Hassanin, Influence of bifilm defects generated during mould filling on the tensile properties of Al–Si–Mg cast alloys. Metals **12**, 160 (2022). https://doi.org/10.3390/met12010160
11. I. Riposan, D. Anca, I. Stan, M. Chisamera, S. Stan, Graphite nodularity evaluation in high-Si ductile cast irons. Materials **15**, 7685 (2022). https://doi.org/10.3390/ma15217685
12. K.M. Pedersen, N.S. Tiedje, Graphite nodule count and size distribution in thin-walled ductile cast iron. Mater. Charact. **59**, 1111–1121 (2008). https://doi.org/10.1016/j.matchar.2007.09.001
13. C. Liu, Y. Du, T. Ying, L. Zhang, X. Zhang, X. Wang, G. Yan, B. Jiang, Effects of graphite nodule count on mechanical properties and thermal conductivity of ductile iron. Mater. Today Commun. **31**, 103522 (2022). https://doi.org/10.1016/j.mtcomm.2022.103522
14. K.D. Millis, A.P. Gagnebin, N.B. Pilling, Gray cast iron having improved properties. US Patent 2,485,761 (filed 22 March 1947, issued 25 October 1949)
15. M. Eissa, H. El-Faramawy, M. Nasr, A. Ahmed, S. Ghali, H. Halfa, M. El-Fawkhry, E. Kotb, An innovative safe process for producing magnesium–ferro–silicon (MgFeSi) alloy containing calcium and rare earth elements. Int. J. Metalcast. **20**, 482–489 (2026). https://doi.org/10.1007/s40962-025-01614-7
16. C. Hartung, D. White, K. Copi, M. Liptak, R. Logan, The continuing evolution of MgFeSi treatments for ductile and CG irons. Int. J. Metalcast. **8**, 7–15 (2014). https://doi.org/10.1007/BF03355577
17. T. Beach, J. Clayton, P. LeBlang, T. Sheets, R. Logan, M. Riabov, J. Morrison, The effects of MgFeSi and inoculant selection on microstructure and mechanical properties of varying section size ductile iron castings. Int. J. Metalcast. **18**, 2022–2035 (2024). https://doi.org/10.1007/s40962-024-01265-0
18. R. Păcurar, P. Berce, O. Nemeş et al., Cast iron parts obtained in ceramic molds produced by binder jetting 3D printing—morphological and mechanical characterization. Materials **14**, 4502 (2021). https://doi.org/10.3390/ma14164502
19. J. Campbell, M. Tiryakioğlu, Bifilm defects in Ni-based alloy castings. Metall. Mater. Trans. B **43**, 902–914 (2012). https://doi.org/10.1007/s11663-012-9655-1
20. M. Dash, M. Makhlouf, Effect of key alloying elements on the feeding characteristics of aluminum–silicon casting alloys. J. Light Met. **1**, 251–265 (2001). https://doi.org/10.1016/S1471-5317(02)00002-0
21. W. Chen, S. Wu, R. Wang, Mechanical wave propagation in solidifying Al-Cu-Mn-Ti alloy and its effect on solidification feeding. Metals **12**, 2001 (2022). https://doi.org/10.3390/met12122001
22. H. Nunes, O. Emadinia, M.F. Vieira, A. Reis, Low- and high-pressure casting aluminum alloys: a review, in *Recent Advancements in Aluminum Alloys* (IntechOpen, London, 2024). https://doi.org/10.5772/intechopen.109869
23. F. Monteiro, G. Soares, R. Madureira et al., Development of the low-pressure die casting process for an aluminium alloy part. Materials **17**, 2835 (2024). https://doi.org/10.3390/ma17122835
24. G.D. Chandley, J.A. Redemske, J.N. Johnson, R.C. Shah, P.H. Mikkola, Counter-gravity casting process for making thinwall steel exhaust manifolds. SAE Technical Paper 970920 (1997). https://doi.org/10.4271/970920
25. G. Ruff, T.E. Prucha, J. Barry, D. Patterson, Pressure counter pressure casting (PCPC) for automotive aluminum structural components. SAE Technical Paper 2001-01-0411 (2001). https://doi.org/10.4271/2001-01-0411
26. EN 1563:2018, *Founding—Spheroidal Graphite Cast Irons* (European Committee for Standardization, Brussels, 2018)
27. ISO 945-4:2019, *Microstructure of Cast Irons—Part 4: Test Method for Evaluating Nodularity in Spheroidal Graphite Cast Irons* (International Organization for Standardization, Geneva, 2019)
28. ISO 945-1:2019, *Microstructure of Cast Irons—Part 1: Graphite Classification by Visual Analysis* (International Organization for Standardization, Geneva, 2019)
29. D.O. Fernandino, R. Boeri, Study of the fracture of ferritic ductile cast iron under different loading conditions. Fatigue Fract. Eng. Mater. Struct. **38**, 610–620 (2015). https://doi.org/10.1111/ffe.12266
30. P.Q. Dai, Z.R. He, C.M. Zheng, Z.Y. Mao, In-situ SEM observation on the fracture of austempered ductile iron. Mater. Sci. Eng. A **319–321**, 531–534 (2001). https://doi.org/10.1016/S0921-5093(01)01088-7

31. F. Iacoviello, O. Di Bartolomeo, V. Di Cocco, V. Piacente, Damaging micromechanisms in ferritic–pearlitic ductile cast irons. Mater. Sci. Eng. A **478**, 181–186 (2008). https://doi.org/10.1016/j.msea.2007.05.110

32. J.H. Zhu, P.K. Liaw, J.M. Corum, J.G.R. Hansen, J.A. Cornie, Damage mechanisms in a cast ductile iron and an Al_2O_{3p}/Al composite. Metall. Mater. Trans. A **29**, 2855–2862 (1998). https://doi.org/10.1007/s11661-998-0326-4